PAPER

Assessing monocyte phenotype in poly(*γ*-glutamic acid) hydrogels formed by orthogonal thiol–norbornene chemistry

IOP Publishing Biomed. Mater. 16 (2021) 045027 https://doi.org/10.1088/1748-605X/ac01b0

Biomedical Materials

PAPER

RECEIVED
18 December 2020

REVISED
4 May 2021

ACCEPTED FOR PUBLICATION
14 May 2021

PUBLISHED
28 May 2021

Assessing monocyte phenotype in poly(γ-glutamic acid) hydrogels formed by orthogonal thiol–norbornene chemistry

Min Hee Kim and Chien-Chi Lin*

Department of Biomedical Engineering, Purdue School of Engineering and Technology, Indiana University-Purdue University Indianapolis, Indianapolis, IN 46202, United States of America

* Author to whom any correspondence should be addressed.

E-mail: lincc@iupui.edu

Keywords: poly(γ-glutamic acid) (γ-PGA), hydrogel, thiol–norbornene click chemistry, 3D encapsulation

Supplementary material for this article is available online

Abstract

Hydrogels with tunable properties are highly desirable in tissue engineering applications as they can serve as artificial extracellular matrix to control cellular fate processes, including adhesion, migration, differentiation, and other phenotypic changes via matrix induced mechanotransduction. Poly(γ-glutamic acid) (PGA) is an natural anionic polypeptide that has excellent biocompatibility, biodegradability, and water solubility. Moreover, the abundant carboxylic acids on PGA can be readily modified to introduce additional functionality or facilitate chemical crosslinking. PGA and its derivatives have been widely used in tissue engineering applications. However, no prior work has explored orthogonal crosslinking of PGA hydrogels by thiol–norbornene (NB) chemistry. In this study, we report the synthesis and orthogonal crosslinking of PGA-norbornene (PGANB) hydrogels. PGANB was synthesized by standard carbodiimide chemistry and crosslinked into hydrogels via either photopolymerization or enzymatic reaction. Moduli of PGA hydrogels were readily tuned by controlling thiol–NB crosslinking conditions or stoichiometric ratio of functional groups. Orthogonally crosslinked PGA hydrogels were used to evaluate the influence of mechanical cues of hydrogel substrate on the phenotype of naïve human monocytes and M0 macrophages in 3D culture.

1. Introduction

Hydrogels are three-dimensional (3D) polymeric matrix crosslinked by physical and/or chemical reactions. The hydrophilic networks of hydrogels provide high water content, tunable viscoelasticity, high permeability, and excellent biocompatibility that are advantageous for various biomedical applications, including tissue regeneration [1–4], drug delivery [5–7], cell therapy [8, 9], and biosensing [10–12]. In particular, hydrogels are increasingly employed to mimic the non-cellular components of the extracellular matrix for studying 3D cell–cell and cell–matrix interactions [13, 14]. For this purpose, hydrogels are often decorated with bioactive molecules, including collagen, laminin, fibronectin, cell-adhesive ligands, proteoglycan (e.g. syndecan, perlecan, hyaluronan, glycosaminoglycan), and protease sensitive motifs for cell-mediated matrix remodeling [15]. Among various hydrogel crosslinking mechanisms, thiol–norbornene (NB) click chemistry is particularly ideal for *in situ* cell encapsulation. These hydrogels can be crosslinked through photopolymerizations or enzymatic reactions between multi-functional NB-functionalized macromer and thiol-containing crosslinkers [16, 17]. In addition, the physiological and biochemical properties of the thiol–NB hydrogels can be readily controlled by adjusting stoichiometric ratio of thiol/NB crosslinkers, by incorporating bioactive peptides (e.g. arg-gly-asp or RGD, matrix metalloproteinase (MMP) sensitive peptides) [3], and by performing post-gelation secondary crosslinking. Hence, thiol–NB hydrogels have been widely used in biomedical applications [18–23].

Poly(γ-glutamic acid) (PGA) is an anionic, naturally occurring polypeptide consists of D-and L-glutamic acid units linked by amide bond between α-amino and γ-carboxylic acid groups. PGA has

excellent biocompatibility, high water solubility, and can be degraded *in vivo* by glutamyl transpeptidase into glutamic acid, making it an attractive material for *in vivo* transplantation [24]. The carboxylic acid groups in the side chain of PGA permit facile bioconjugation for introducing functional moieties for network crosslinking and bioactive modification. PGA and its derivatives have been widely used in the fields of drug delivery [25, 26], wound dressing [27], and tissue engineering [28–30]. For example, Gao *et al* synthesized pH-responsive injectable PGA via conjugating 3-glycidoxypropyl trimethoxysilane (GPTMS) [25]. The sol–gel transition occurred through forming Si–O–Si bond by a condensation reaction between silanol groups of GPTMS and TEOS in a biological environment. Yang *et al* synthesized thiol- and glycidyl methacrylate-modified PGA for gelation via thiol-Michael addition reaction, which occurred rapidly under physiological condition and the material was used for promoting cartilage regeneration [31]. In a separate example, mussel-inspired catechol (Cat) was introduced into the PGA side chains and the macromer PGA-Cat was crosslinked into adhesive hydrogels via horseradish peroxidase (HRP) mediated oxidation [32]. Nonetheless, modular crosslinking of PGA hydrogels with orthogonal thiol–NB chemistry has not been reported in the literature.

Circulating in the blood, monocytes are recruited to the site of injury/disease to regulate local inflammatory response. Once differentiated, monocytes-derived macrophages are responsible for regulating local inflammation induced by infections, injuries, and other foreign objects (e.g. implants) via phagocytic activity and secretion of pro-inflammatory and anti-inflammatory cytokines [33]. THP-1 is a human leukemia monocyte cell line that can be differentiated into macrophage-like cells when treated with phorbol esters [34]. Differentiated THP-1 cells behave similar to natural monocyte-derived macrophages and are increasingly used as a cell model to study inflammatory response [35]. Recent studies have investigated the adaptation of macrophage cellular behavior in responding to the changes of physicochemical properties of hydrogels. For example, the effect of substrate stiffness on THP-1 cell polarization was evaluated using collagen-coated polyacrylamide hydrogels [36]. It was demonstrated that cells cultured on the surface of stiff gels ($E \sim 323$ kPa) polarized into a pro-inflammatory phenotype (M1) with impaired phagocytic activity. On the other hand, THP-1 cells cultured on lower stiffness hydrogels ($E \sim 11$–88 kPa) were primed towards an anti-inflammatory phenotype (M2). In another example, Cha *et al* compared different hydrogels on THP-1 cell polarization in 3D. Specifically, THP-1 cells were encapsulated in either gelatin-based or poly(ethylene glycol) diacrylate (PEGDA) hydrogels with shear moduli (G') of ∼25 kPa. Interestingly, THP-1 cells encapsulated within PEGDA hydrogel lacking cell attachment motif yielded pro-inflammatory M1 macrophages, whereas gelatin-based hydrogels induced an anti-inflammatory M2-like phenotype [37]. Other recent studies have also shown that gelatin and hyaluronic acid based 3D culture of THP-1 cells promoted their differentiation into pro-inflammatory macrophages [38, 39]. Nevertheless, the effect of matrix stiffness on macrophage activity in 3D condition has not been extensively studied.

In this study, we report the synthesis and characterization of PGA-norbornene (PGANB) and its orthogonal crosslinking into PGA hydrogels via thiol–NB click chemistry. Carboxylic acids on PGA was chemically modified with NB moieties through standard carbodiimide chemistry using 5-norbornene-2-methylaime. Orthogonal crosslinking of PGA hydrogels was achieved either through light-initiated or enzyme-mediated thiol–NB click chemistry [16, 40–42]. Similar to other modularly crosslinked hydrogels, PGA hydrogel crosslinking can be tuned by controlling thiol/NB ratio, functionality thiol crosslinker, and polymer contents. Furthermore, we exploited the unique HRP-mediated thiol–NB gelation chemistry to form enzymatically crosslinked PGA hydrogels. Finally, we assessed the effect of matrix stiffness on viability, polarization, and cytokine secretion of THP-1 cells encapsulated in highly tunable PGA hydrogels.

2. Experimental

2.1. Materials

High molecular weight poly(γ-glutamic acid) (γ-PGA, Mw 1000 000 Da) was obtained from Vedan Corp (Taiwan). Dithiothreitol (DTT) was purchased from Fisher Scientific. Four-arm-PEG-SH (PEG4SH) was purchased from Laysan Bio, Inc. Lithium phenyl-2,4,6-trimethylbenzoylphosphinate (LAP) was purchased from Sigma Aldrich. 1-(3-Dimethylaminopropyl)-3-ethylcarbodiimide hydrochloride (EDC) was purchased from Accros Organics and N-hydroxysuccinimide (NHS) and 5-norbornene-2-methylamine were purchased from Tokyo Chemical Industry Co., Ltd. All reagents were used as received without further purification.

2.2. Synthesis of norbornene modified poly(γ-glutamic acid) (PGANB)

PGANB was synthesized by modifying γ-PGA with 5-norbornene-2-methylamine using EDC/NHS chemistry. Briefly, 1 g of γ-PGA (7.7 mmol of –COOH) was dissolved in 100 ml MES buffer (pH 6.0) to obtain 1 wt% solution. EDC (5 mmol) and NHS (5 mmol) were then added to the γ-PGA solution and stirred for 1 h, after which 5-norbornene-2-methylamine

(3.85 mmol) was added and the reaction was allowed to continue for 24 h. PGANB was purified by dialysis against water for four days with decreasing NaCl gradient from 150 mM to 0 mM using cellulose dialysis membrane (cut-off 12 000–13 000). The final product was lyophilized for four days. The NB conjugated PGANB was characterized using proton nuclear magnetic resonance (^{1}H NMR, 500 MHz, ADVANCE III, Bruker, USA). ^{1}H NMR was used to confirm the structural change, and the degree of catechol substitution (DS, %) was defined as a number of substituents (signals at δ 6.0 ppm, NB proton) per 100 carboxyl groups in γ-PGA backbone (δ 3.9–4.3, 1.8–2.7 ppm, α-proton of γ-PGA) as calculated using the following equation (1)

$$\text{Degree of norbornene substitution } (\%) = \frac{A_f/2}{(A_a + A_b + A_c)/5} \times 100. \quad (1)$$

2.3. Synthesis and characterization of heparin conjugated PGANB (PGANB_Hep)

PGANB_Hep was synthesized by clicking tetrazine modified-heparin (Hep-Tz) to PGANB. Hep-Tz was synthesized following a previously reported method [43]. Tz:NB ratio was fixed at 0.05 and components were mixed for 1 h. In order to determine the Tz-NB clickable reaction, absorbance at 523 nm was measured using a microplate reader (Synergy HT, BioTek). Dimethyl methylene blue (DMMB) assay was further used to qualitatively detect the immobilization of heparin within PGANB hydrogels. Briefly, DMMB reagent was prepared by adding 16 mg DMMB zinc chloride into 1 l of double distilled water containing 3.04 g glycine, 1.6 g sodium chloride, and 95 ml of 0.1 M acetic acid. PGANB hydrogels with or without heparin modification were then immersed in 2 ml of DMMB solutions and incubated at room temperature for 24 h. After which, gels were transferred to PBS to remove residual DMMB solution, and the gels were washed to PBS for 1 h, followed by imaging with a digital camera [19].

2.4. Hydrogel fabrication and characterization

The PGANB hydrogels were fabricated by reacting PGANB and DTT or PEG4SH via thiol–NB click chemistry. Photo-crosslinked PGANB hydrogels were crosslinked by mixing PGANB with sulfhydryl-containing crosslinkers at a unity stoichiometric ratio of thiol to NB along with photoinitiator LAP (1 mM). The precursor solution with pre-defined compositions was injected between two glass slides separated by 1 mm Teflon spacers, followed by exposure to 365 nm light (5 mW cm^{-2}) for 2 min. In order to prepare the enzyme-mediated PGANB hydrogel, 5 wt% PGANB and thiol-crosslinkers (DTT or PEG4SH) were mixed at a stoichiometric ratio of thiol to NB along with HRP (50–400 U ml^{-1}). Gelation was initiated by adding H_2O_2 (0.5–1.5 mM) to the precursor solution.

In situ gelation studies were conducted using an oscillatory rheometer (Bohlin CVO 100). Briefly, PGA-NB solution containing thiol cross-linkers and photoinitiator LAP (or HRP/H_2O_2 in enzymatic crosslinking) were mixed and vortexed for 5 s. Immediately after vortexing, 8 µl of the mixture was placed on the lower plate and the geometry was lowered to 90 µm and *in situ* rheometry was performed in time sweep mode (0.5% strain at 1 Hz) at 25 °C. To prevent gel from drying, the rim of the geometry was sealed with mineral oil. For light-mediated gelation, UV light was turned on 10 s after starting the measurement. Hydrogel shear moduli were measured using circular hydrogel discs fabricated between two glass slides. Gel discs were punched out with an 8 mm biopsy punch after 24 h incubation in PBS at 37 °C. The hydrogels were carefully transferred to the rheometer prior to initiating the measurements and the frequency-sweep test was conducted at 1% strain.

In order to study the swelling kinetics, PGA hydrogels were crosslinked and dried, followed by incubation in pH 7.4 PBS at room temperature. At predetermined intervals, the swollen gels were weighed after blotting to remove the adhering excess water. The swelling ratio of PGANB hydrogels was calculated using the following equation:

$$\text{Swelling ratio } (\%) = (W_t - W_d)/W_d \times 100 \quad (2)$$

where W_d and W_t are the weights of dried hydrogel and swollen gel at time t, respectively. The equilibrium swelling ratio was determined at the point which no further weight change was detected.

2.5. Quantification of H_2O_2 and thiol levels

For enzymatic PGA hydrogel crosslinking using HRP, hydrogen peroxide levels in the pre-gel solution were quantified with a QuantiChrom TM Peroxide assay kit (BioAssay Systems). Briefly, 40 µl of PGANB pre-gel solution (5 wt% PGANB with DTT, $R = 0.8$) with different HRP concentration was mixed with 200 µl reagent and evaluated in 96 well plates using the manufacturer's protocol, and absorbance at 585 nm was monitored.

The degree of thiol consumption in the presence of NB/HRP solution were quantified using Ellman's assay. Briefly, predetermined DTT/HRP solution was mixed with non-gelling macromer solution containing linear methoxyl-PEG-NB with DTT (6 wt%, $R = 0.8$). Samples were taken at regular intervals and the leftover thiol contents were determined using the Ellman's reagent.

2.6. Growth factor absorption test

Thermostable recombinant basic fibroblast growth factor (bFGF-G3, acquired from the Recombinant

Protein Production Core, Northwestern University) was used for growth factor absorption study. PGANB hydrogel were photo-polymerized and immersed in buffer containing bFGF (3 ng ml^{-1}) at 37 °C. The vials were placed on an orbital shaker at 100 rpm and sampled at pre-determined time intervals. The collected samples were stored at −80 °C prior to determining concentrations using human bFGF-basic standard ABTS ELISA kits (Peprotech) according to manufacturer's protocol.

2.7. Cell culture and encapsulation

Human monocyte cell line THP-1 was generously provided by Professor Heiko Konig (Indiana University School of Medicine). THP-1 cells were maintained in RPMI-1640 supplemented with 10% fetal bovine serum and 1% penicillin-streptomycin. Media was refreshed every two to three days. THP-1 cells were encapsulated in PGANB hydrogels at 2×10^6 cells ml^{-1}. Alternatively, THP-1 cells were differentiated to M0 macrophages by treating the cells in serum-free media containing Phorbol 12-myristate 13-acetate (PMA, 20 ng ml^{-1}) for 24 h. The cells were mixed with sterile-filtered (0.22 μm) pre-polymer solutions containing PGANB, DTT or PEG4SH, and LAP (1 mM). The solution was mixed and pipetted into a 1 ml syringe with cut-open tip. Cell-laden gels were formed upon exposure to 365 nm light (5 mW cm^{-2}) for 2 min and were placed in a non-treated 24-well plate with fresh media. At pre-determined time periods (day 2, 4, 7 and 10), cell-laden hydrogels were collected and characterized for their viability and morphology. Cell-laden hydrogels were also stained with Live/Dead kit, as well as antibodies for CCR7 (ThermoFisher Scientific) and CD36 (Santa Cruz Biotechnology). Samples were imaged by confocal microscopy (Olympus Fluoview FV100).

2.8. Cytokine secretion

The cytokines secreted by THP-1 cells and M0 macrophages were detected using Human Cytokine array C3 kit (Raybiotech). THP-1 cells were encapsulated and cultured in PGANB hydrogel with different stiffness. Cells cultured in 24 well plates were used for 2D control. After incubation for four days, cell culture media were collected and added to the membrane which was blocked by the blocking buffer and incubated overnight at 4°C. After washing, the membranes were incubated with biotinylated antibody cocktail overnight at 4 °C, followed by incubation with diluted HRP-streptavidin overnight at 4°C. After further washing, 500 μl of detection buffer mixture was added to each membrane, incubated for 2 min at room temperature, and imaged. The secretion of inflammatory cytokine interleukin (IL)-8 was furthered verified using a standard ELISA kit (Peprotech).

2.9. Statistical analysis

All statistical analyses were performed using GraphPad Prism 8 software. Significance comparison between experimental groups was performed using two-way ANOVA with Bonferroni's post testing. All experiments were conducted a minimum of three times with data presentation as the mean ± standard error of the mean. One, two, or three asterisks represent $p < 0.05$, 0.01, or 0.001, respectively.

3. Results and discussion

3.1. Synthesis of PGANB and light-mediated gelation

PGANB was synthesized by grafting the carboxylate groups of γ-PGA with 5-norbrnene-2-methylamine using carbodiimide chemistry with EDC and NHS as the coupling reagents (figure 1(A)). Successful NB modification was determined using ^{1}H NMR. Unmodified γ-PGA has four major signals at 2.11, 2.25, 2.53 and 4.32 ppm, which represent the protons of β-CH_2, γ-CH_2 and α-CH, respectively. Signals at δ 5.8–6.3 ppm represent the unsaturated proton peak on NB (figure S1 (available online at stacks.iop.org/BMM/16/045027/mmedia)), indicating that the γ-PGA was successfully modified. The DS was calculated to be about 5.4% relative to the total carboxylic acid units. This degree of modification was sufficient for crosslinking linear PGA into a hydrogel network owing to its high molecular weight (1000 000 Da) and water solubility.

Similar to other NB-modified polymers, PGANB could be orthogonally cross-linked with various thiol-bearing cross-linkers into hydrogels. In this study, we used two different thiol crosslinkers (DTT and PEG4SH) to prepare orthogonally crosslinked PGANB hydrogels with different stiffness. Using *in situ* photo-rheometry, we demonstrated a rapid thiol–NB gelation kinetics of PGANB and DTT. Specifically, light-mediated sol–gel transition occurred quickly (gel point ∼10 s) and reached completion within 30 s, which was on par with other UV light initiated thiol–NB gelation system (figure 1(B)) [3]. The gelation rate was not significantly affected by stoichiometric ratio of thiol-to-NB ([SH]/[NB] or $R_{thiol/NB}$) (figure S2(A)). However, adjusting $R_{thiol/NB}$ from 0.2 to 1.0 led to increased gel cross-linking density and shear moduli (∼150–1300 Pa for [SH]/[NB] of 0.2–1.0 figure 1(C)). At the same PGANB weight content, gel moduli could also be controlled by using thiol-bearing cross-linkers with different functionality (e.g. two for DTT or four for PEG4SH) where the use of DTT led to gels with G′ of ∼1 kPa (named as soft) and the use of PEG4SH resulted in gels with G′ of ∼5.8 kPa (named as stiff) (figure 1(D)). On the other hand, as PGANB concentration was raised from 3 to 7 wt%, the stiffness of the hydrogels was increased from 0.25 kPa to ∼3 kPa (figure S2(B)).

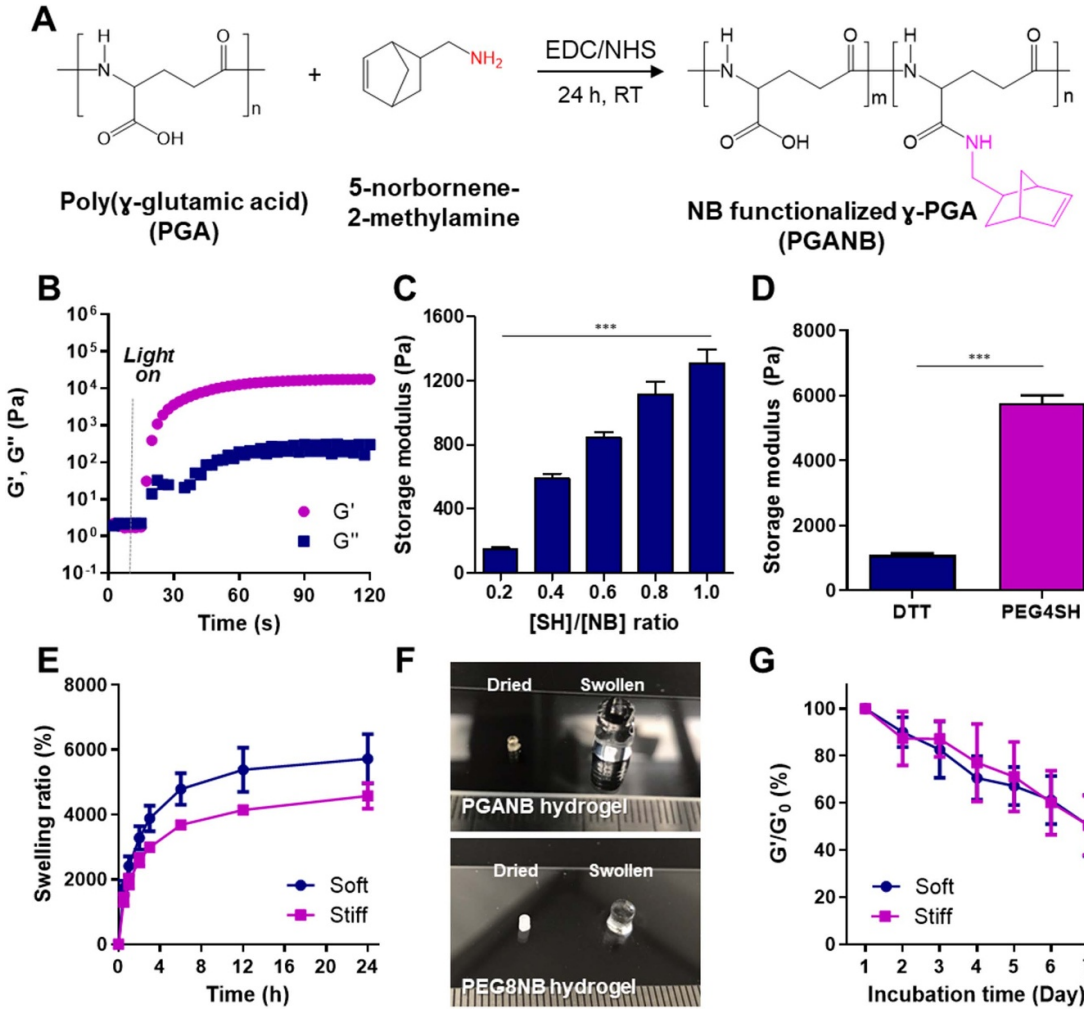

Figure 1. Synthesis and crosslinking of PGANB hydrogels. (A) Schematic of PGANB synthesis. (B) *In situ* photorheometry of PGANB hydrogel crosslinking (5 wt% PGANB with DTT, $R_{thiol/NB} = 0.8$, 1 mM LAP, 2 min light). Effects of (C) [SH]/[NB] (or $R_{thiol/NB}$) and (D) thiol cross-linker on hydrogel stiffness. (E) Swelling behavior of PGANB hydrogels. (F) Photographs of dried and swollen hydrogels crosslinked by PGANB (top) and PEG8NB (bottom). DTT ($R = 0.8$) was used as the crosslinker in both groups. (G) Hydrolytic degradation of PGANB hydrogels ($n \geqslant 5$).

The swelling property of PGANB hydrogels was investigated by measuring changes in their weights during 24 h of incubation (figure 1(E)). PGANB-DTT hydrogels absorbed significant amount of water and reached equilibrium states within 12 h (e.g. 5722% for soft hydrogel and 4574% for stiff hydrogel, respectively figures 1(E) and (F)). As a comparison, we fabricated similar hydrogels with 5 wt% of eight-arm PEG-norbornene (PEG8NB) and found that the swelling of PEG8NB-DTT hydrogels (swelling ratio: 1666 ± 119%) was much lower than that of PGANB-DTT hydrogels. The high water imbibing nature of PGANB hydrogels rendered it an ideal matrix to mimic wound exudate, a swollen inflammatory site where macrophages would reside and function. In addition to swelling, the degradation kinetics is another critical parameter when designing hydrogels for biomedical applications. We noted that PGANB hydrogels degraded overtime even in the absence of protease (i.e. in PBS, figure 1(G)). The stiffness of PGANB hydrogels decreased ∼50% over seven days of incubation regardless of cross-linker type. Since NB was conjugated on PGA via a hydrolytically stable amide bond, the hydrolytic degradation of PGANB hydrogels likely occurred at the PGA backbone.

3.2. Heparinization and growth factor absorption in PGANB hydrogels

In order to enhance the bioactive property of PGANB hydrogel, we further modified PGANB with heparin, a glycosaminoglycan that sequesters a wide range of growth factors. Heparin was first modified with tetrazine-amine (Tz-amine, Click Chemistry Tools) following a published protocol [43], yielding heparin-tetrazine (Hep-Tz). Hep-Tz was readily 'clicked' to PGANB through an inverse electron-demand Diels-Alder (iEDDA) reaction (figure 2(A)), which has been increasingly used in functionalization of biomaterials owing to its rapid reaction kinetics, mild reaction conditions, and non-toxic reaction by-product (i.e., N_2 gas). Successful heparinization was confirmed using DMMB, which complexes with heparin to

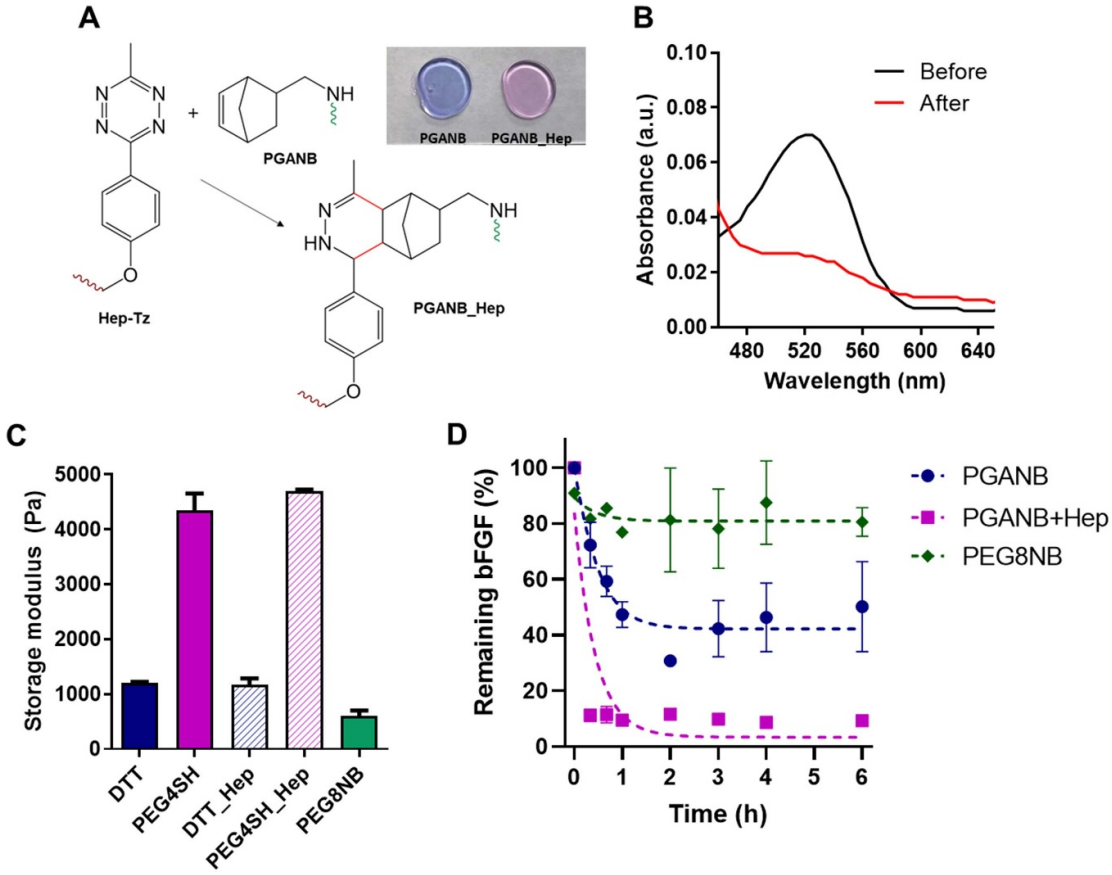

Figure 2. Heparinization of PGANB hydrogels. (A) Schematic of iEDDA click reaction between Hep-Tz and PGANB. Inlet image represents the DMMB qualitative assay to verify immobilization of heparin within the PGANB_Hep hydrogels. (B) UV–vis spectra of PGANB_Hep before and after reaction with PGANB. (C) Stiffness of 5 wt% PGANB or PGANB_Hep hydrogels crosslinked by different crosslinkers. PEG8NB was sued as control. (D) Effect of heparinization on growth factor absorption.

induce color change from blue to pink that occurred only in the PGANB_Hep hydrogels (figure 2(A), inlet image). The NB-Tz click reaction was monitored via measuring absorbance at 523 nm using a microplate reader. After 1 h of reaction, it was confirmed that the Tz absorbance peak disappeared and the color of PGANB/Hep-Tz solution changed from pink to yellow (figure 2(B)). Furthermore, heparin-modification did not alter the degree of hydrogel crosslinking regardless of the crosslinker used and there was no significant difference in gel stiffness after Hep modification for both sets of gels ($G' \sim 1.2$ kPa and ~4.4 kPa for DTT and PEG4SH, respectively, figure 2(C)). Hydrogel crosslinked by PEG8NB and DTT were used as control ($G' \sim 0.7$ kPa). However, heparin modification did improve growth factor sequestration in PGANB hydrogels. Using a thermal-stable bFGF-G3, which can be detected using conventional bFGF ELISA kit (figures S3 and S4), we showed that significantly more bFGF (~89%) was adsorbed in the PGANB-Hep gel than PGANB gels (~50%) (figure 2(D)). Interestingly, even the non-heparinized PGANB hydrogels showed significantly higher growth factor absorption than the relatively inert PEG-based hydrogels (3 wt% PEG8NB with DTT, $R = 1$). This was likely due to electrostatic interaction between the positively charged bFGF and the carboxylic acid moieties in the PGA chain, as well as the high level of swelling of PGANB hydrogels. It is expected that this hydrogel formulation should have broader impact on supporting cell fate processes in 3D due to the broad affinity of heparin to various growth factors and cell-secreted cytokines.

3.3. Enzyme-mediated crosslinking of PGANB hydrogels

Our group has recently shown that thiol–NB hydrogel crosslinking can be initiated not only by photopolymerization but also by enzymatic reaction, hence permitting injectable delivery of thiol–NB hydrogels [16]. We tested whether PGANB hydrogels could also be crosslinked using the same enzymatic reaction. Figure 3(A) shows that mixture of PGANB, DTT, and HRP/H_2O_2 resulted in a viscous polymer solution (blue dye added for visualization), which could also be injected through a syringe. Figure 3(B) further demonstrates *in situ* gelation kinetic of enzymatically crosslinked PGANB hydrogels using DTT or PEG4SH as the crosslinker. Not surprisingly, the use of tetra-functional PEG4SH led to faster G'–G'' crossover. However, the gelation rate of enzyme-mediated PGANB hydrogel crosslinking

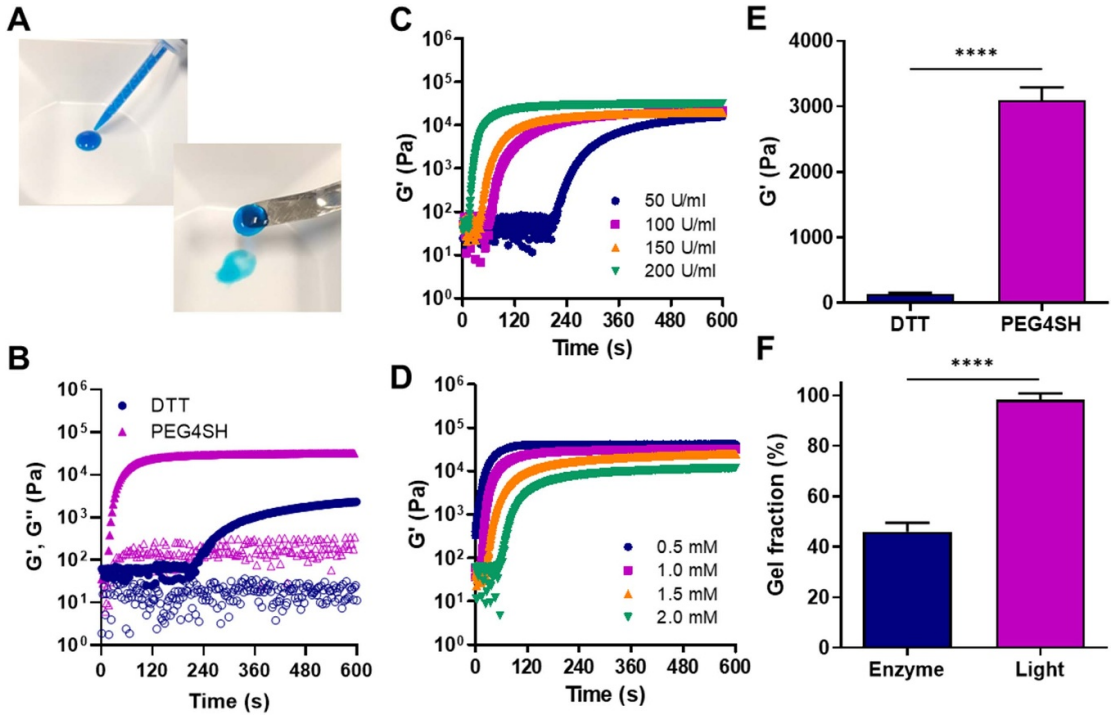

Figure 3. Enzyme-mediated gelation of PGANB hydrogel. (A) Digital images on injected PGANB hydrogels using dual syringe (5 wt% PGANB with PEG4SH, $R = 0.8$, 200 U ml^{-1} HRP and 1 mM H_2O_2). (B) *In situ* rheometry of HRP-mediated gelation of PGANB (5 wt%) with DTT or PEG4SH ($R_{thiol/NB} = 0.8$, 200 U ml^{-1} HRP and 1 mM H_2O_2). (C) and (D) Effect of HRP (C) H_2O_2 (D) on gelation kinetics. (E) and (F) Shear moduli (E) and gel fraction (F) of PGANB hydrogels crosslinked by DTT or PEG4SH.

was slightly slower than that of light-mediated gelation (218 s vs 32 s, respectively). The gelation kinetics were also affected by HRP and H_2O_2 concentrations (figures 3(C) and (D)). Specifically, gel point was accelerated from 203 s to 10 s as the concentration of HRP was increased from 50 to 200 U ml^{-1}. Interestingly, the gelation was found to be slowed down as the concentration of H_2O_2 increased from 0.5 mM to 2 mM, most likely due to inhibition of the HRP activity at an elevated H_2O_2 content [44].

Similar to results shown in figure 1(D), the shear moduli of the enzyme-crosslinked PGANB hydrogels were influenced by the type of thiol crosslinkers (figure 3(E)). However, it appeared that the shear moduli of enzyme-crosslinked PGANB hydrogels were lower than that formed by photopolymerization. To confirm that enzymatic crosslinking led to lower crosslinking efficiency, we measured the gel fraction of PGANB hydrogels crosslinked by either enzymatic reaction or photopolymerization (figure 3(F)). Clearly, the gel fractions of the photopolymerized PGANB hydrogels were significantly higher than that crosslinked by enzymatic reaction.

While moderate level of exogenous H_2O_2 accelerated HRP-mediated gelation (figure 3(D)), we found that PGANB hydrogel could slowly reach sol–gel transition (~21 min) even in the absence of H_2O_2 (figure 4(A)). We hypothesized that H_2O_2 was generated during the preparation of pre-gel solution due to the self-oxidation between the thiol group on the crosslinker and HRP [45]. To test this hypothesis, we mixed all macromer components necessary for gelation except H_2O_2. We then quantified the changes in H_2O_2 concentration over time. The concentration of H_2O_2 in the solution containing no thiol cross-linker (i.e. DTT) was relatively unchanged over 1 h regardless of HRP concentration (figure 4(B)). However, notable H_2O_2 accumulation was detected in the presence of DTT and in an HRP concentration dependent manner (figure 4(B)). We also evaluated oxygen and free sulfhydryl concentrations in the reaction and found that both decreased with time upon adding HRP (figures 4(C) and (D)). We reasoned that self-crosslinking was achieved through the self-oxidation of free sulfhydryl groups, which was promoted by adding thiol crosslinker and/or increasing HRP concentration (figure 4(E)). Oxygen was consumed during the self-oxidation, leading to endogenous H_2O_2 production to activate HRP for initiating the thiol–NB crosslinking. Our results were in agreement with studies by Gantumur *et al*, where mixture of alginate derivative possessing phenolic hydroxyl moieties and HRP yielded a hydrogel without adding oxidation reagent such as H_2O_2. This reason was explained as the generation of H_2O_2 by self-oxidation of thiol present in HRP. In our study, macroscopic PGANB hydrogels were crosslinked slowly though HRP-mediated crosslinking in the absence of exogenously added H_2O_2. The lower gel fraction observed in the HRP-mediated

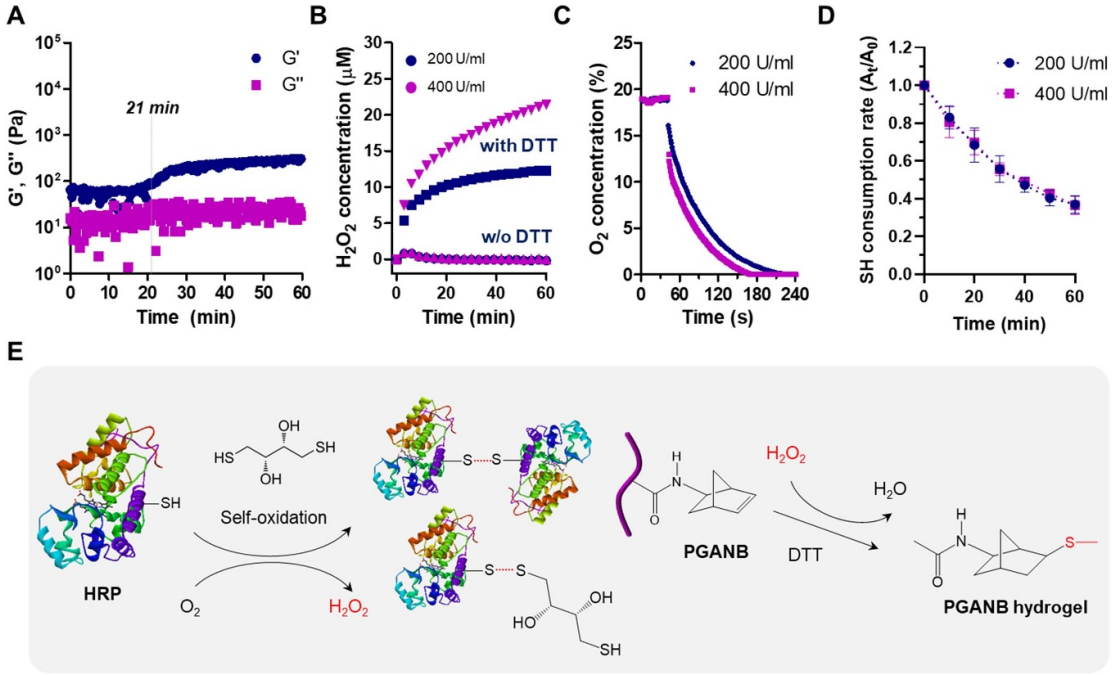

Figure 4. Enzyme-mediated gelation of PGANB hydrogel free of exogenous addition of H_2O_2. (A) *In situ* rheometry of PGANB-DTT hydrogels with 200 U ml^{-1} HRP and no exogenous H_2O_2. (B) H_2O_2 production in PGANB solution in the presence or absence of DTT. (C) Oxygen consumption in PGANB solution. In (A)–(C): PGANB: 5 wt%, $R_{thiol/NB} = 0.8$. (D) Thiol consumption in the presence of mono-functional PEGNB (6 wt%) and HRP (200–400 U ml^{-1}) without exogenous H_2O_2. (E) Potential mechanism of HRP-mediated thiol–norbornene cross-linking of PGANB hydrogel without exogenous H_2O_2.

crosslinking could be due to the partial self-oxidation of the thiol groups. Nonetheless, the results reported here established the potential of using enzymatic reaction to fabricate injectable and modularly crosslinked PGA hydrogels.

3.4. 3D cell culture and polarization

The highly swollen PGA hydrogels were used as a 3D culture matrix to study how matrix stiffness would affect phenotype of naïve human monocytes THP-1 cells and M0 macrophages primed by treating the cells with PMA for 24 h. Cells were encapsulated and cultured in PGANB hydrogel crosslinked with MMP-degradable peptide linker supplemented with DTT (soft gels) or PEG4SH (stiff gels) and immobilized with integrin ligand RGD. Figure 5 shows that the majority of the encapsulated THP-1 cells and M0 macrophages were viable post-encapsulation, regardless of hydrogel stiffness. Upon detailed examination of cell viability using confocal microscopy, we found that both THP-1 cells and M0 macrophages encapsulated in the softer PGANB hydrogels proliferated into small clusters over the seven day culture period. However, this was not observed in the stiff gels, where dead cells were visible (figure S3). The high cell viability of THP-1 cells in soft hydrogels was attributed to the compliant and low crosslinking density of the network, which exerted lower constrain and stress to the encapsulated cells.

Immunostaining for macrophage subtype markers revealed qualitative differences of the encapsulated cells depending on the hydrogel stiffness (figure 6(A)). Results showed that both native THP-1 cells and PMA-primed M0 macrophage were stained positive for both M1 and M2 polarization markers (i.e. CCR7 as an M1 marker and CD36 as an M2 marker). However, 3D encapsulation in stiff PGANB hydrogels led to higher level of CCR7 positive cells and less for the M2 marker, CD36. In contrast, in soft hydrogel, encapsulated cells showed enhanced positive staining for CD36 and less positive staining for CCR7. In order to further evaluate the effect of matrix stiffness on secretory profiles from THP-1 cells, we collected the conditioned media and detected the secretion of 42 inflammatory cytokines using an antibody array kit. No significance difference was found in 22 of the 42 cytokines (figure S4). The remaining 20 proteins were classified into M1 (pro-inflammatory) and M2 (anti-inflammatory) related cytokines [46]. The levels of cytokines secreted from 2D culture were also assayed as controls. As shown in figure 6(B), the secretion of M1-related cytokines in 3D cultured THP-1 cells were mostly increased compare to 2D culture despite the excellent protein absorption ability of PGANB hydrogels (figure 2(D)). However, compared with 2D culture, the secretions of some cytokines from THP-1 cells were reduced in 3D culture, including

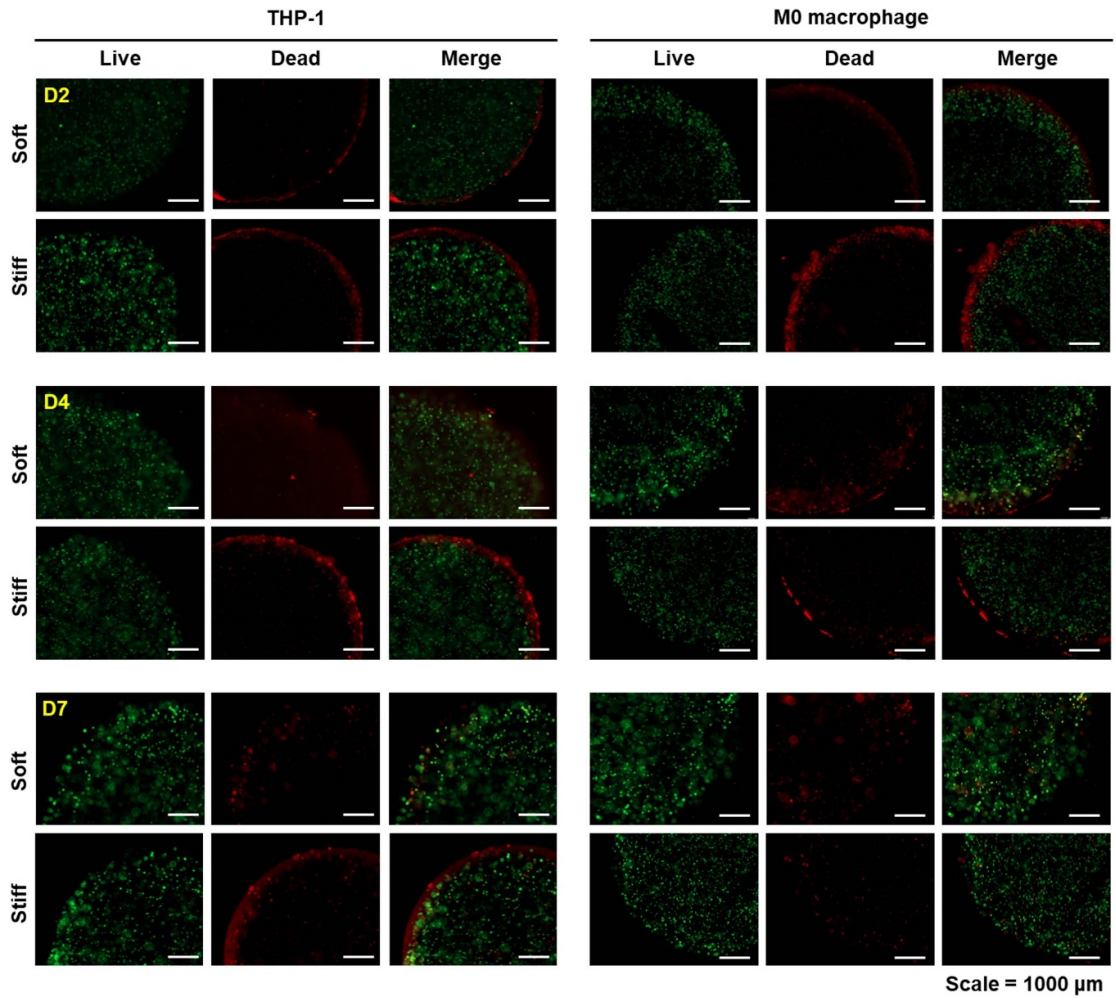

Figure 5. Representative live/dead staining of the encapsulated THP-1 cells and M0 macrophages in PGANB hydrogels with difference stiffness.

IL-1α, IL-1β, IL-15, interferon-γ (IFN-γ), granulocyte colony stimulating factor, RANTES, and vascular endothelial growth factor (VEGF). Interestingly, the secretions of some key cytokines from THP-1 cells were significantly upregulated in both soft and stiff hydrogels than in 2D culture, including IL-8, MCP-1, MCP-3, tumor necrosis factor α (TNFα), and TNFβ. In the encapsulated THP-1 cells, the secretions of M2-related cytokines were slightly upregulated in 3D hydrogel culture, but the levels were relatively lower when compared with M1 related cytokines. For both THP-1 cells and M0 macrophages, expression of M2 associated cytokines (e.g. IL-4, IL-12p40, IL-13 and EGF) were slightly higher in softer gels than in stiffer matrix (figure 6(B)). For the encapsulated M0 macrophages, cytokine secretions were mostly increased in 3D hydrogel culture, except for RANTES. Antibody-based cytokine array is a Western blot-like qualitative assay that permits rapid identification of cytokines that were differentially secreted when the cells were cultured in different microenvironments. To quantitatively verify the results, we used ELISA, a more sensitive and quantitative assay, to detect the secretion of IL-8, which was highly expressed in stiff hydrogels. Figure 6(C) shows that, when compared with 2D culture, pro-inflammatory IL-8 levels increased rapidly from 3D culture over time, especially in stiffer PGANB hydrogels. Of note, both the cytokine array and the ELISA results shown in figure 6 were performed without taking into account the variation of cell viability in 3D hydrogels (figure 5). This means that the differences in IL-8 secretion would have been more drastic on a per-cell basis between the three culture conditions.

Recent studies have shown that the 3D microenvironment could induce M1 polarization of macrophages [38, 47]. Our results showed that both THP-1 cells and M0 macrophages polarized with PMA exhibited similar cytokine secretion behavior and that 3D hydrogel culture increased the production of pro-inflammatory cytokines. Our study also showed that M1-like macrophages were induced by stiffer 3D microenvironment, which is consistent with the literature [38, 47]. Interestingly, pre-differentiation of THP-1 cells into M0 macrophages changed the secretion profiles when the cells were cultured on 2D but it

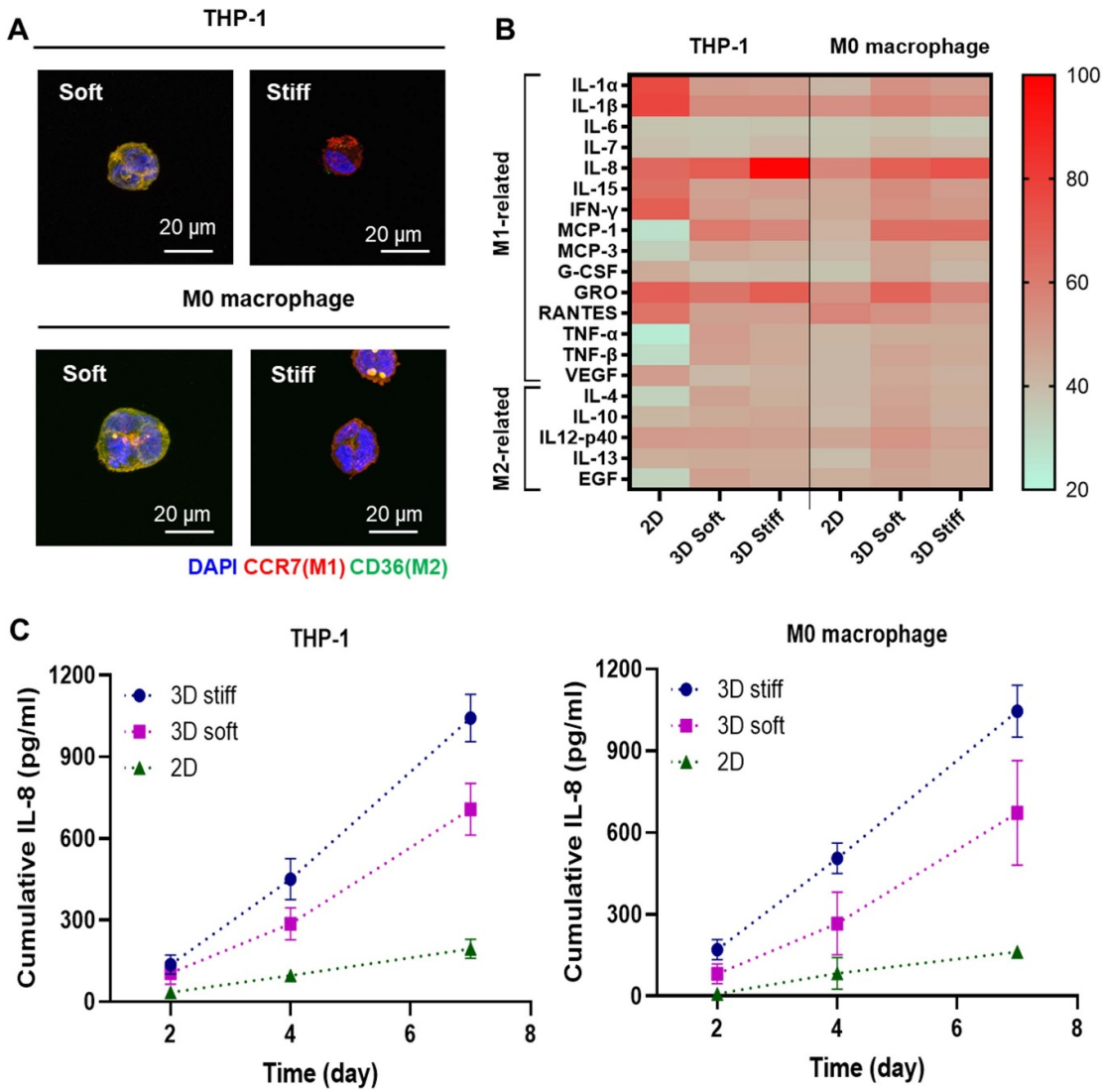

Figure 6. Cytokine secretion from THP-1 cells and M0 macrophages cultured in 2D, soft, and stiff PGANB hydrogels. (A) Immunostaining for polarization markers expressed in THP-1 cells and M0 macrophages at day 7. (B) Heat-map of M1 and associated cytokines measured by human cytokine array C3 kit using conditioned media collected on day 4 of culture. Results were shown as adjusted mean volume (OD × mm^2) ± SD of two repeats on the antibody membranes. The average intensity of the pixels in background volume was calculated and subtracted from each pixel in all standard and samples using ImageJ. (C) ELISA measurement of secreted IL-8.

did not prime the cells to produce different secretion profiles in 3D hydrogels, suggesting that 3D hydrogels may be more effective in priming the monocytes into different phenotypes.

In general, IFN-γ/LPS treated pro-inflammatory M1 macrophages upregulate expression of TNF-α, IL-1β, IL-6, IL-8, MCP-1, LOX, and Leptin. In anti-inflammatory M2 macrophages polarized by IL-4/IL-13, secretion of MCP-1 was shown to be decreased, which was accompanied with increased expression of anti-inflammatory cytokine (e.g. IL-12p40, IL-23) and CD36 [48–50]. Furthermore, unlike IL-8, the detected levels of M1-related cytokine secretion, including TNF-α, IL-1β, and IL-6 were relatively low. It was possible that these cytokines were retained in the PGA hydrogels owing to their excellent protein absorption property [51]. IL-8, MCP-1, IL-12p40 are upregulated when NF-κB signaling is activated in THP-1 cells. On the other hand, IL-12p40 acts as a chemoattractant for macrophages and promote the migration of dendritic cells [51–53]. Therefore, we hypothesized that matrix stiffness could modulate the immune response through the toll-like receptor 4 (TLR4) signal transduction pathway, which leads to the activation of NF-κB. In stiff matrix, TLR pathway activates the transcription of genes encoding inflammatory cytokines such as IL-8, MCP-1, and GRO by inducing nuclear translocation of NF-κB [33, 54, 55]. Furthermore, recent study has shown that IL-8 secretion was increased in TLR-2 and TLR-4 stimulated undifferentiated THP-1cells [56]. We hypothesize that human monocyte and M0 macrophages encapsulated in stiff hydrogel were activated toward M1 macrophage. On the other hand, in soft matrix, TLR signaling induces expression of IL-12p40 through the activation of another transcription

factor, interferon-regulatory factor 3 and led to M2 macrophage-like behavior [52]. Future work will focus on using this hydrogel platform for macrophage/fibroblast co-culture model to investigate the effect of cytokine stimulation by matrix stiffness on regulation of inflammatory response.

4. Conclusions

In summary, natural polypeptide-based hydrogels consisting of NB functionalized PGA were fabricated via orthogonal thiol–NB chemistry. By using crosslinking reaction between NB and variety of thiol crosslinkers with different initiation methods (i.e. photopolymerization and enzymatic reaction), physical/biochemical properties of the PGA hydrogels could be readily controlled. Furthermore, bioactive property of the hydrogel was enhanced through Tz-NB clickable reaction. PGANB hydrogels exhibited excellent swelling properties and high protein absorption ability compared to PEG-based hydrogel. PGANB hydrogels also displayed excellent cytocompatibility for human monocyte cells encapsulation but higher gel stiffness may lead to gradual loss of cell viability death while promoting M1 polarization. The tunable physicochemical properties of orthogonally crosslinked PGANB hydrogels may serve as a promising biomaterial platform for 3D cell culture.

Data availability statement

All data that support the findings of this study are included within the article (and any supplementary files).

Acknowledgments

This work was supported in part by the National Cancer Institute (R01CA227737) and Walther Cancer Foundation via an Oncology Physical Sciences and Engineering Research Embedding Program Award.

ORCID iD

Chien-Chi Lin https://orcid.org/0000-0002-4175-8796

References

[1] Ahearne M, Yang Y, El Haj A J, Then K Y and Liu K-K 2005 Characterizing the viscoelastic properties of thin hydrogel-based constructs for tissue engineering applications *J. R. Soc. Interface* **2** 455–63
[2] Wang H and Heilshorn S C 2015 Adaptable hydrogel networks with reversible linkages for tissue engineering *Adv. Mater.* **27** 3717–36
[3] Lin C C, Ki C S and Shih H 2015 Thiol–norbornene photoclick hydrogels for tissue engineering applications *J. Appl. Polym. Sci.* **132** 41563
[4] Lee K Y and Mooney D J 2001 Hydrogels for tissue engineering *Chem. Rev.* **101** 1869–80
[5] Qiu Y and Park K 2001 Environment-sensitive hydrogels for drug delivery *Adv. Drug Deliv. Rev.* **53** 321–39
[6] Hoare T R and Kohane D S 2008 Hydrogels in drug delivery: progress and challenges *Polymer* **49** 1993–2007
[7] Li J and Mooney D J 2016 Designing hydrogels for controlled drug delivery *Nat. Rev. Mater.* **1** 1–17
[8] Nguyen Q V, Park J H and Lee D S 2015 Injectable polymeric hydrogels for the delivery of therapeutic agents: a review *Eur. Polym. J.* **72** 602–19
[9] DeForest C A and Anseth K S 2012 Advances in bioactive hydrogels to probe and direct cell fate *Annu. Rev. Chem.* **3** 421–44
[10] Ullah F, Othman M B H, Javed F, Ahmad Z and Akil H M 2015 Classification, processing and application of hydrogels: a review *Mater. Sci. Eng.* C **57** 414–33
[11] Buenger D, Topuz F and Groll J 2012 Hydrogels in sensing applications *Prog. Polym. Sci.* **37** 1678–719
[12] le Goff G C, Srinivas R L, Hill W A and Doyle P S 2015 Hydrogel microparticles for biosensing *Eur. Polym. J.* **72** 386–412
[13] Wong S W, Lenzini S, Cooper M H, Mooney D J and Shin J-W 2020 Soft extracellular matrix enhances inflammatory activation of mesenchymal stromal cells to induce monocyte production and trafficking *Sci. Adv.* **6** eaaw0158
[14] Shin J-W and Mooney D J 2016 Extracellular matrix stiffness causes systematic variations in proliferation and chemosensitivity in myeloid leukemias *Proc. Natl Acad. Sci. USA* **113** 12126–31
[15] Chen X D, Dusevich V, Feng J Q, Manolagas S C and Jilka R L 2007 Extracellular matrix made by bone marrow cells facilitates expansion of marrow-derived mesenchymal progenitor cells and prevents their differentiation into osteoblasts *J. Bone Miner. Res.* **22** 1943–56
[16] Nguyen H D, Liu H-Y, Hudson B N and Lin C-C 2019 Enzymatic cross-linking of dynamic thiol-norbornene click hydrogels *ACS Biomater. Sci. Eng.* **5** 1247–56
[17] Fairbanks B D, Schwartz M P, Halevi A E, Nuttelman C R, Bowman C N and Anseth K S 2009 A versatile synthetic extracellular matrix mimic via thiol-norbornene photopolymerization *Adv. Mater.* **21** 5005–10
[18] Gramlich W M, Kim I L and Burdick J A 2013 Synthesis and orthogonal photopatterning of hyaluronic acid hydrogels with thiol-norbornene chemistry *Biomaterials* **34** 9803–11
[19] Greene T and Lin C-C 2015 Modular cross-linking of gelatin-based thiol–norbornene hydrogels for *in vitro* 3D culture of hepatocellular carcinoma cells *ACS Biomater. Sci. Eng.* **1** 1314–23
[20] Ki C S, Lin T-Y, Korc M and Lin C-C 2014 Thiol-ene hydrogels as desmoplasia-mimetic matrices for modeling pancreatic cancer cell growth, invasion, and drug resistance *Biomaterials* **35** 9668–77
[21] McCall J D and Anseth K S 2012 Thiol–ene photopolymerizations provide a facile method to encapsulate proteins and maintain their bioactivity *Biomacromolecules* **13** 2410–7
[22] Highley C B, Song K H, Daly A C and Burdick J A 2019 Jammed microgel inks for 3D printing applications *Adv. Sci.* **6** 1801076
[23] Song K H, Highley C B, Rouff A and Burdick J A 2018 Complex 3D-printed microchannels within cell-degradable hydrogels *Adv. Funct. Mater.* **28** 1801331
[24] Feng J, Gao W, Gu Y, Zhang W, Cao M, Song C, Zhang P, Sun M, Yang C and Wang S 2014 Functions of poly-gamma-glutamic acid (γ-PGA) degradation genes in γ-PGA synthesis and cell morphology maintenance *Appl. Microbiol. Biotechnol.* **98** 6397–407
[25] Gao Q, Zhang C, Wang M, Wu Y, Gao C and Zhu P 2020 Injectable pH-responsive poly (γ-glutamic acid)-silica hybrid hydrogels with high mechanical strength, conductivity and cytocompatibility for biomedical applications *Polymer* **197** 122489

[26] Bae H H, Cho M Y, Hong J H, Poo H, Sung M-H and Lim Y T 2012 Bio-derived poly (gamma-glutamic acid) nanogels as controlled anticancer drug delivery carriers *J. Microbiol. Biotechnol.* **22** 1782–9
[27] Tsao C T, Chang C H, Lin Y Y, Wu M F, Wang J L, Young T H, Han J L and Hsieh K H 2011 Evaluation of chitosan/γ-poly (glutamic acid) polyelectrolyte complex for wound dressing materials *Carbohydr. Polym.* **84** 812–9
[28] Hua J, Li Z, Xia W, Yang N, Gong J, Zhang J and Qiao C 2016 Preparation and properties of EDC/NHS mediated crosslinking poly (gamma-glutamic acid)/epsilon-polylysine hydrogels *Mater. Sci. Eng.* C **61** 879–92
[29] Liu S, Pu Y, Yang R, Liu X, Wang P, Wang X, Ren Y, Tan X, Ye Z and Chi B 2020 Boron-assisted dual-crosslinked poly (γ-glutamic acid) hydrogels with high toughness for cartilage regeneration *Int. J. Biol. Macromol.* **153** 158–68
[30] Gonçalves R M, Antunes J C and Barbosa M A 2012 Mesenchymal stem cell recruitment by stromal derived factor-1-delivery systems based on chitosan/poly (gamma-glutamic acid) polyelectrolyte complexes *Eur. Cells Mater.* **23** 249–60
[31] Yang R, Wang X, Liu S, Zhang W, Wang P, Liu X, Ren Y, Tan X and Chi B 2020 Bioinspired poly (γ-glutamic acid) hydrogels for enhanced chondrogenesis of bone marrow-derived mesenchymal stem cells *Int. J. Biol. Macromol.* **142** 332–44
[32] Kim M H, Lee J N, Lee J, Lee H and Park W H 2020 Enzymatically crosslinked poly (γ-glutamic acid) hydrogel with enhanced tissue adhesive property *ACS Biomater. Sci. Eng.* **6** 3103–33
[33] Previtera M L and Sengupta A 2015 Substrate stiffness regulates proinflammatory mediator production through TLR4 activity in macrophages *PLoS One* **10** e0145813
[34] Ubanako P, Xelwa N and Ntwasa M 2019 LPS induces inflammatory chemokines via TLR-4 signalling and enhances the Warburg effect in THP-1 cells *PLoS One* **14** e0222614
[35] Grim J C, Aguado B A, Vogt B J, Batan D, Andrichik C L, Schroeder M E, Gonzalez-Rodriguez A, Yavitt F M, Weiss R M and Anseth K S 2020 Secreted factors from proinflammatory macrophages promote an osteoblast-like phenotype in valvular interstitial cells *Arterioscler. Thromb. Vasc. Biol.* **40** e296–e308
[36] Sridharan R, Cavanagh B, Cameron A R, Kelly D J and O'Brien F J 2019 Material stiffness influences the polarization state, function and migration mode of macrophages *Acta Biomater.* **89** 47–59
[37] Cha B H *et al* 2017 Integrin-mediated interactions control macrophage polarization in 3D hydrogels *Adv. Healthcare Mater.* **6** 1700289
[38] Bhattacharya A, Agarwal M, Mukherjee R, Sen P and Sinha D K 2018 3D micro-environment regulates NF-κβ dependent adhesion to induce monocyte differentiation *Cell Death Dis.* **9** 1–16
[39] Bystroňová J, Ščigalková I, Wolfová L, Pravda M, Vrana N E and Velebný V 2018 Creating a 3D microenvironment for monocyte cultivation: ECM-mimicking hydrogels based on gelatine and hyaluronic acid derivatives *RSC Adv.* **8** 7606–14
[40] Shih H, Liu H-Y and Lin C-C 2017 Improving gelation efficiency and cytocompatibility of visible light polymerized thiol-norbornene hydrogels via addition of soluble tyrosine *Biomater. Sci.* **5** 589–99
[41] Shih H, Greene T, Korc M and Lin C-C 2016 Modular and adaptable tumor niche prepared from visible light initiated thiol-norbornene photopolymerization *Biomacromolecules* **17** 3872–82
[42] Mũnoz Z, Shih H and Lin C-C 2014 Gelatin hydrogels formed by orthogonal thiol–norbornene photochemistry for cell encapsulation *Biomater. Sci.* **2** 1063–72
[43] Peuler K, Dimmitt N and Lin C-C 2020 Clickable modular polysaccharide nanoparticles for selective cell-targeting *Carbohydr. Polym.* **234** 115901
[44] Malomo S O, Adeoye R I, Babatunde L, Saheed I A, Iniaghe M O and Olorunniji F J 2011 Suicide inactivation of horseradish peroxidase by excess hydrogen peroxide: the effects of reaction pH, buffer ion concentration, and redox mediation *Biokemistri* **23** 124–8
[45] Gantumur E, Sakai S, Nakahata M and Taya M 2017 Cytocompatible enzymatic hydrogelation mediated by glucose and cysteine residues *ACS Macro Lett.* **6** 485–8
[46] Tedesco S, de Majo F, Kim J, Trenti A, Trevisi L, Fadini G P, Bolego C, Zandstra P W, Cignarella A and Vitiello L 2018 Convenience versus biological significance: are PMA-differentiated THP-1 cells a reliable substitute for blood-derived macrophages when studying *in vitro* polarization? *Front. Pharmacol.* **9** 71
[47] Lee S and Ki C S 2020 Inflammatory responses of macrophage-like RAW264.7 cells in a 3D hydrogel matrix to ultrasonicated schizophyllan *Carbohydr. Polym.* **229** 115555
[48] Garcia-Sabaté A, Mohamed W K E, Sapudom J, Alatoom A, Al Safadi L and Teo J 2020 Biomimetic 3D models for investigating the role of monocytes and macrophages in atherosclerosis *Bioengineering* **7** 113
[49] Lee K Y 2019 M1 and M2 polarization of macrophages: a mini-review *Med. Biol. Sci. Eng.* **2** 1–5
[50] Zhang Y, Böse T, Unger R E, Jansen J A, Kirkpatrick C J and van den Beucken J J 2017 Macrophage type modulates osteogenic differentiation of adipose tissue MSCs *Cell Tissue Res.* **369** 273–86
[51] Li J, Qin Y, Chen Y, Zhao P, Liu X, Dong H, Zheng W, Feng S, Mao X and Li C 2020 Mechanisms of the lipopolysaccharide-induced inflammatory response in alveolar epithelial cell/macrophage co-culture *Exp. Ther. Med.* **20** 1–10
[52] Takeuchi O 2012 IRF3: a molecular switch in pathogen responses *Nat. Immunol.* **13** 634–5
[53] Cooper A M and Khader S A 2007 IL-12p40: an inherently agonistic cytokine *Trends Immunol.* **28** 33–38
[54] Ishihara S, Yasuda M, Harada I, Mizutani T, Kawabata K and Haga H 2013 Substrate stiffness regulates temporary NF-κB activation via actomyosin contractions *Exp. Cell Res.* **319** 2916–27
[55] Irwin E, Saha K, Rosenbluth M, Gamble L, Castner D and Healy K E 2008 Modulus-dependent macrophage adhesion and behavior J *J. Biomater. Sci. Polym. Ed.* **19** 1363–82
[56] Pinto S, Kim H, Subbannayya Y, Giambelluca M, Bösl K and Kandasamy R K 2020 Dose-dependent phorbol 12-myristate-13-acetate-1 mediated monocyte-to-macrophage differentiation induces unique proteomic signatures in THP-1 cells (BioRxiv 968016)